ICASSP 2021 - 2021 IEEE International Conference on Acoustics, Speech and Signal Processing (ICASSP) | 978-1-7281-7605-5/20/$31.00 ©2021 IEEE | DOI: 10.1109/ICASSP39728.2021.9414025

PROBABILITY OF RESOLUTION OF G-MUSIC: AN ASYMPTOTIC APPROACH

David Schenck[⋆] *Xavier Mestre*[‡] *Marius Pesavento*[⋆]

[⋆]Communication Systems Group, Technische Universität Darmstadt, Germany
[‡]Centre Tecnològic de Telecomunicacions de Catalunya, Castelldefels, Spain

ABSTRACT

In this paper, the outlier production mechanism of the G-MUSIC Direction-of-Arrival estimation technique is investigated using tools from Random Matrix Theory. The G-MUSIC Direction-of-Arrival estimation technique is an improved version of the conventional MUSIC method that provides superior performance in low sample size scenarios. The stochastic behavior of the G-MUSIC cost function is analyzed in the asymptotic regime where both the number of snapshots and the number of antennas increase without bound at the same rate. The finite dimensional distribution of the G-MUSIC cost function is shown to be asymptotically jointly Gaussian. Furthermore, the probability of resolution of the G-MUSIC Direction-of-Arrival estimator is characterized by means of the derived asymptotic probability density function of the G-MUSIC cost function.

***Index Terms*—** Direction-of-Arrival Estimation, G-MUSIC, Central Limit Theorem, Random Matrix Theory

1. INTRODUCTION

Direction-of-Arrival (DoA) estimation is a highly relevant area of research as it is commonly used in a vast variety of applications such as e.g. in radar, sonar, mobile communications, seismic exploration and electric surveillance [1–3]. Several DoA estimation algorithms have been proposed and analyzed in the literature. Among them, high resolution subspace-based algorithms that provide a good compromise between DoA estimation accuracy and computational complexity. Subspace-based algorithms do not require computational expensive multidimensional spectral search and still provide reasonable performance. The Multiple Signal Classification (MUSIC) DoA estimation method is among the most popular subspace-based algorithms as it is widely used in praxis [4]. However, the MUSIC method suffers from a rapid performance breakdown if either the number of snapshots or the Signal-to-Noise Ratio (SNR) falls below a certain threshold, which is often referred to as the threshold effect [5, 6]. The G-MUSIC DoA estimation technique is a modified version of the MUSIC method which was introduced to improve the performance in low sample size scenarios where the number of snapshots is comparable in magnitude to the number of sensors [7]. In comparison to the MUSIC method, the G-MUSIC DoA estimation technique provides higher resolution capabilities and improved DoA estimation accuracy in particular in low-sample size scenarios with closely spaced signals [7].

The performance analysis of the conventional MUSIC method has received a lot of attention in the literature [8–14]. However, most of the performance analyses rely on traditional asymptotics where the number of snapshots increases without bound whereas the number of sensors remains fixed. Nonetheless, in many practical use cases the number of snapshots is comparable in magnitude to the number of sensors which makes asymptotic analysis under the assumption that the number of snapshots and the number of sensors tend to infinity at the same rate particularly appealing. In [15] the asymptotic behavior of the DoA estimates of the MUSIC method as well as the G-MUSIC method was studied under the latter asymptotic scenario. However, the asymptotic stochastic behavior of the MUSIC and G-MUSIC cost function has received little attention up to now.

The main objective of this paper is the performance characterization of the G-MUSIC technique in the threshold region, whereby both the SNR and the number of samples per antenna take moderate values. This region is typically characterized by a systematic appearance of outliers in the DoA estimates which are caused by merging signal extrema in the spectrum of the DoA estimator. In order to study the probability of resolution of the G-MUSIC technique we follow a similar approach as in [16–18] and [19, 20] where the probability of resolution of the recently introduced Partially Relaxed Deterministic Maximum Likelihood (PR-DML) algorithm and the conventional Deterministic Maximum Likelihood (DML) as well as the Stochastic Maximum Likelihood (SML) method was derived using tools from Random Matrix Theory (RMT). Whereas the PR-DML, the DML and the SML DoA estimation techniques only involve eigenvalues in the computation of the cost function, the cost function of the G-MUSIC technique also involves eigenvectors and therefore requires a fundamentally new asymptotic stochastic analysis. The stochastic behavior of the G-MUSIC cost function is analyzed in the asymptotic scenario where the number of snapshots and the number of sensors tend to infinity at the same rate. In contrast to [21] where the asymptotic variance of the G-MUSIC cost function was studied we consider the more general case of the covariance and show that the G-MUSIC cost function is asymptotically jointly Gaussian distributed.

This paper is organized as follows. The system model is provided in Section 2 followed by the G-MUSIC DoA estimation technique in Section 3. In Section 4 the asymptotic behavior of the G-MUSIC cost function is provided. A sketch of the corresponding proof is given in Section 5. The probability of resolution is introduced in Section 6 and simulation results are provided in Section 7. Section 8 concludes this paper.

2. SIGNAL MODEL

Let us consider an antenna array that is equipped with M sensors and K impinging narrowband signals such that $M>K$. The DoAs that correspond to the K sources are denoted by $\boldsymbol{\theta}=[\theta_1,...,\theta_K]^{\mathrm{T}}$ and placed within the Field of View (FoV) Θ of the sensor array.

This work was supported in part by the DFG PRIDE Project PE 2080/2-1, the German Academic Exchange Service, the Catalan Government under grant 2017-SGR-01479 and the Spanish Government under grant RTI2018-099722-B-I00.

The transmitted signals at time instant n are denoted by $\boldsymbol{s}(n)=[s_1(n),...,s_K(n)]^{\mathrm{T}}$. Furthermore, the full-rank steering matrix is given by $\boldsymbol{A}(\boldsymbol{\theta})=[\boldsymbol{a}(\theta_1),...,\boldsymbol{a}(\theta_K)]\in\mathbb{C}^{M\times K}$ where $\boldsymbol{a}(\theta_i)\in\mathbb{C}^M$ denotes the sensor array response of the i-th impinging signal. The received baseband signal $\boldsymbol{x}(n)\in\mathbb{C}^M$ at the n-th time instant is given by

$$\boldsymbol{x}(n)=\boldsymbol{A}(\boldsymbol{\theta})\boldsymbol{s}(n)+\boldsymbol{n}(n),\quad n=1,...,N, \tag{1}$$

where $\boldsymbol{n}(n)\in\mathbb{C}^M$ denotes the sensor noise and N the number of snapshots. Assuming that signal and noise variables are statistically independent zero-mean circularly Gaussian distributed, the covariance matrix of the received signal $\boldsymbol{R}\in\mathbb{C}^{M\times M}$ is given by

$$\boldsymbol{R}=\mathbb{E}\Big\{\boldsymbol{x}(n)\boldsymbol{x}(n)^{\mathrm{H}}\Big\}=\boldsymbol{A}\boldsymbol{R}_{\mathrm{s}}\boldsymbol{A}^{\mathrm{H}}+\sigma^2\boldsymbol{I}_M, \tag{2}$$

where $\boldsymbol{R}_{\mathrm{s}}=\mathbb{E}\{\boldsymbol{s}(n)\boldsymbol{s}(n)^{\mathrm{H}}\}\in\mathbb{C}^{K\times K}$ denotes the covariance matrix of the transmitted signal and $\sigma^2\boldsymbol{I}_M$ is the noise covariance matrix. The distinct eigenvalues of the covariance matrix $\boldsymbol{R}$ in (2) are sorted in ascending order and denoted by $\gamma_1<\gamma_2<\cdots<\gamma_{\bar{M}}$, where $\bar{M}$ is the number of distinct eigenvalues ($1\leq\bar{M}\leq M$). Each eigenvalue γ_m has multiplicity K_m for $m=1,...,\bar{M}$ such that $\sum_{m=1}^{\bar{M}}K_m=M$. Furthermore, there exists a complex subspace $\boldsymbol{E}_m$ of dimensions $M\times K_m$ that is associated to each eigenvalue γ_m for $m=1,...,\bar{M}$ such that $\boldsymbol{E}_m^{\mathrm{H}}\boldsymbol{E}_m=\boldsymbol{I}_{K_m}$. Hence, the covariance matrix in (2) can equivalently be expressed as

$$\boldsymbol{R}=\sum_{m=1}^{\bar{M}}\gamma_m\boldsymbol{E}_m\boldsymbol{E}_m^{\mathrm{H}}=\boldsymbol{E}\begin{bmatrix}\gamma_1\boldsymbol{I}_{K_1} & & \\ & \ddots & \\ & & \gamma_{\bar{M}}\boldsymbol{I}_{K_{\bar{M}}}\end{bmatrix}\boldsymbol{E}^{\mathrm{H}},$$

where $\boldsymbol{E}=[\boldsymbol{E}_1,...,\boldsymbol{E}_{\bar{M}}]\in\mathbb{C}^{M\times M}$. Furthermore, $\boldsymbol{U}_{\mathrm{n}}=\boldsymbol{E}_1$ is referred to as the noise subspace whereas $\boldsymbol{U}_{\mathrm{s}}=[\boldsymbol{E}_2,...,\boldsymbol{E}_{\bar{M}}]$ is referred to as the signal subspace, respectively. Since the true covariance matrix in (2) is unavailable in practice, the sample covariance matrix

$$\hat{\boldsymbol{R}}=\frac{1}{N}\sum_{n=1}^{N}\boldsymbol{x}(n)\boldsymbol{x}(n)^{\mathrm{H}}, \tag{3}$$

is used instead. The eigenvalues of the sample covariance matrix in (3) are sorted in non-descending order $\hat{\lambda}_1\leq\hat{\lambda}_2\leq\cdots\leq\hat{\lambda}_M$ and referred to as sample eigenvalues. Associated to each sample eigenvalue $\hat{\lambda}_m$ there exists a sample eigenvector $\hat{\boldsymbol{e}}_m\in\mathbb{C}^M$, for $m=1,...,M$, such that

$$\hat{\boldsymbol{R}}=\hat{\boldsymbol{E}}\begin{bmatrix}\hat{\lambda}_1 & & \\ & \ddots & \\ & & \hat{\lambda}_M\end{bmatrix}\hat{\boldsymbol{E}}^{\mathrm{H}},$$

where $\hat{\boldsymbol{E}}=[\hat{\boldsymbol{e}}_1,...,\hat{\boldsymbol{e}}_M]$. The sample noise subspace is denoted by $\hat{\boldsymbol{U}}_{\mathrm{n}}=[\hat{\boldsymbol{e}}_1,...,\hat{\boldsymbol{e}}_{M-K}]$ and the sample signal subspace is given by $\hat{\boldsymbol{U}}_{\mathrm{s}}=[\hat{\boldsymbol{e}}_{M-K+1},...,\hat{\boldsymbol{e}}_M]$. The asymptotic behavior of $\hat{\boldsymbol{R}}$ in (3) is discussed next.

2.1. Assumptions and Random Matrix Theory Preliminaries

According to the law of large numbers for finite M, $\hat{\boldsymbol{R}}\to\boldsymbol{R}$ almost surely as $N\to\infty$, where the convergence is considered for any matrix norm, e.g. $\|\boldsymbol{R}-\hat{\boldsymbol{R}}\|_{\mathrm{F}}\to0$ [22]. However, in practice the number of snapshots N is limited and comparable in magnitude to the number of snapshots M which results in a poorly estimated covariance matrix in the sense that $\|\boldsymbol{R}-\hat{\boldsymbol{R}}\|_{\mathrm{F}}$ is far away from zero [22]. Therefore, we consider the realistic case where M and N are large but comparable in magnitude. In fact, we concentrate on the asymptotic case where $M,N\to\infty$ at the same rate and their ratio $M/N\to c$ converges to a fixed finite quantity $0<c<\infty$ [23]. The covariance matrix $\boldsymbol{R}$ in (2) is assumed to have uniformly bounded spectral norm for all M. Furthermore, the sample covariance matrix in (3) can equivalently be expressed as $\hat{\boldsymbol{R}}=\boldsymbol{R}^{1/2}\frac{\boldsymbol{Z}\boldsymbol{Z}^{\mathrm{H}}}{N}\boldsymbol{R}^{\mathrm{H}/2}$, where $\boldsymbol{Z}$ is a $M\times N$ matrix of i.i.d. Gaussian random variables with law $\mathcal{CN}(0,1)$.

Under all the previously mentioned assumptions the empirical eigenvalue distribution of $\hat{\boldsymbol{R}}$ in (3) is almost surely close to a non-random distribution which is absolutely continuous with density $q_M(x)$ [24–26]. With increasing number of snapshots N and therefore decreasing c, $q_M(x)$ tends to concentrate around the distinct eigenvalues of the true covariance matrix $\boldsymbol{R}$ forming different clusters. The number of eigenvalue clusters increases with decreasing c as clusters begin to split. For sufficiently small c there exist exactly as many clusters as true and distinct eigenvalues resulting in a bijective correspondence between sample eigenvalue clusters and distinct eigenvalues. Hence, for sufficiently small c it is possible to assign the sample eigenvalues that belong to the same cluster to one particular true and distinct eigenvalue and vice versa [23]. Assuming there are S distinct clusters, the support of the non-random eigenvalue density $q_M(x)$ is given by the set of S disjoint compact intervals $\mathcal{S}=[x_1^-,x_1^+]\cup\cdots\cup[x_S^-,x_S^+]$. In order to distinguish between noise and signal subspace it is crucial that the cluster $[x_1^-,x_1^+]$ that is associated to the distinct noise eigenvalue γ_1 is well separated from the cluster associated to γ_2 in the asymptotic eigenvalue density $q_M(x)$. Whether there exists separation between the clusters associated to γ_1 and γ_2 depends on the ratio between the number of antennas and the number of snapshots M/N, the SNR as well as the DoAs $\boldsymbol{\theta}$ [23]. The G-MUSIC DoA estimation technique is introduced next.

3. G-MUSIC

The conventional high resolution MUSIC DoA estimation technique utilizes the fact that any vector lying on the signal subspace is orthogonal to the columns of the noise subspace $\boldsymbol{U}_{\mathrm{n}}$ [4, 7]. Hence, the DoAs are estimated by searching for the K arguments in θ such that the array steering vector $\boldsymbol{a}(\theta)$ lies on the signal subspace $\boldsymbol{U}_{\mathrm{s}}$ of $\boldsymbol{R}$ or, equivalently by searching for the values of θ such that $\eta(\theta)=0$ [7], where

$$\eta(\theta)=\boldsymbol{a}(\theta)^{\mathrm{H}}\boldsymbol{U}_{\mathrm{n}}\boldsymbol{U}_{\mathrm{n}}^{\mathrm{H}}\boldsymbol{a}(\theta). \tag{4}$$

In practice $\boldsymbol{U}_{\mathrm{n}}$ is unknown and estimated using the sample noise subspace $\hat{\boldsymbol{U}}_{\mathrm{n}}$. Hence, the conventional MUSIC cost function is obtained by replacing the noise subspace $\boldsymbol{U}_{\mathrm{n}}$ in (4) with its sample estimate $\hat{\boldsymbol{U}}_{\mathrm{n}}$ according to

$$\tilde{\eta}(\theta)=\boldsymbol{a}(\theta)^{\mathrm{H}}\hat{\boldsymbol{U}}_{\mathrm{n}}\hat{\boldsymbol{U}}_{\mathrm{n}}^{\mathrm{H}}\boldsymbol{a}(\theta), \tag{5}$$

and the DoAs are determined by searching for the K deepest local minima of the cost function $\tilde{\eta}(\theta)$ in (5) [4]. However, the conventional MUSIC cost function $\tilde{\eta}(\theta)$ in (5) only provides a good estimate on $\eta(\theta)$ in (4) if the number of snapshots is much larger than the number of sensors $N\gg M$ as $|\eta(\theta)-\tilde{\eta}(\theta)|\to0$ for $N\to\infty$ and fixed finite $M<\infty$ [7]. For the practically important case where M and N are large but comparable in magnitude $\tilde{\eta}(\theta)$ is a bad estimate for $\eta(\theta)$ in the sense that $|\eta(\theta)-\tilde{\eta}(\theta)|$ is far away from zero. The G-MUSIC cost function $\hat{\eta}(\theta)$ was developed in [7] to provide a consistent estimate on $\eta(\theta)$ in (4) in the asymptotic case where $M,N\to\infty$ at the same rate ($M/N\to c$, $0<c<\infty$) such that

$$|\eta(\theta)-\hat{\eta}(\theta)|\to0,\text{ for } M,N\to\infty. \tag{6}$$

The G-MUSIC cost function yields

$$\hat{\eta}(\theta)=\sum_{m=1}^{M}\phi(m)\boldsymbol{a}(\theta)^{\mathrm{H}}\hat{\boldsymbol{e}}_m\hat{\boldsymbol{e}}_m^{\mathrm{H}}\boldsymbol{a}(\theta) \tag{7}$$

with real-valued weights

$$\phi(m)=\begin{cases}1+\sum_{k=M-K+1}^{M}\left(\frac{\hat{\lambda}_k}{\hat{\lambda}_m-\hat{\lambda}_k}-\frac{\hat{\mu}_k}{\hat{\lambda}_m-\hat{\mu}_k}\right), & m\leq M-K,\\ -\sum_{k=1}^{M-K}\left(\frac{\hat{\lambda}_k}{\hat{\lambda}_m-\hat{\lambda}_k}-\frac{\hat{\mu}_k}{\hat{\lambda}_m-\hat{\mu}_k}\right), & m>M-K,\end{cases}$$

where $\hat{\mu}_1\leq\hat{\mu}_2\leq\cdots\leq\hat{\mu}_M$ are the real-valued solutions to the following equation in $\hat{\mu}$

$$\frac{1}{M}\sum_{k=1}^{M}\frac{\hat{\lambda}_k}{\hat{\lambda}_k-\hat{\mu}}=\frac{1}{c}.$$

The DoAs are estimated by searching for the K deepest separable local minima of the cost function $\hat{\eta}(\theta)$ in (7). It was shown in [7] and [15] that the G-MUSIC DoA estimation technique provides higher DoA estimation accuracy compared to the conventional MUSIC method especially in scenarios with small sample sizes. Furthermore, let $\boldsymbol{\eta}(\bar{\boldsymbol{\theta}})$ and $\hat{\boldsymbol{\eta}}(\bar{\boldsymbol{\theta}})$ denote two $L\times 1$ real-valued vectors

$$\boldsymbol{\eta}(\bar{\boldsymbol{\theta}})=\left[\eta(\bar{\theta}_1),...,\eta(\bar{\theta}_L)\right]^{\mathrm{T}}, \tag{8}$$

$$\hat{\boldsymbol{\eta}}(\bar{\boldsymbol{\theta}})=\left[\hat{\eta}(\bar{\theta}_1),...,\hat{\eta}(\bar{\theta}_L)\right]^{\mathrm{T}}, \tag{9}$$

obtained from (4) and (7) respectively, where $\bar{\boldsymbol{\theta}}=[\bar{\theta}_1,...,\bar{\theta}_L]^{\mathrm{T}}$ denotes a set of L distinct points within the FoV Θ of the sensor array. In the following the asymptotic stochastic behavior of the G-MUSIC cost function vector in (9) is studied.

4. MAIN RESULT: ASYMPTOTIC BEHAVIOR

Theorem 1. *Under all the previously mentioned assumptions and as $M,N\to\infty$ at the same rate ($M/N\to c$, $0<c<\infty$) the random vector*

$$\sqrt{N}\left(\hat{\boldsymbol{\eta}}(\bar{\boldsymbol{\theta}})-\boldsymbol{\eta}(\bar{\boldsymbol{\theta}})\right)\to\mathcal{N}\left(\boldsymbol{0},\boldsymbol{\Gamma}(\bar{\boldsymbol{\theta}})\right), \tag{10}$$

converges in distribution to a multivariate Gaussian distribution with zero mean and covariance matrix $\boldsymbol{\Gamma}(\bar{\boldsymbol{\theta}})\in\mathbb{R}^{L\times L}$ with elements

$$\left[\boldsymbol{\Gamma}(\bar{\boldsymbol{\theta}})\right]_{p,q}=\sum_{r=1}^{\bar{M}}\sum_{k=1}^{\bar{M}}\xi(r,k)\boldsymbol{a}(\bar{\theta}_p)^{\mathrm{H}}\boldsymbol{E}_r\boldsymbol{E}_r^{\mathrm{H}}\boldsymbol{a}(\bar{\theta}_q)\boldsymbol{a}(\bar{\theta}_q)^{\mathrm{H}}\boldsymbol{E}_k\boldsymbol{E}_k^{\mathrm{H}}\boldsymbol{a}(\bar{\theta}_p) \tag{11}$$

for $p,q\in\{1,...,L\}$ where the coefficients $\xi(r,k)$ are given by

$$\xi(r,k)=-\frac{N}{K_1}\delta_{r=k=1}+\frac{2}{\pi}\int_{x_1^-}^{x_1^+}\frac{\gamma_r\gamma_k|\omega'(x)|^2\mathrm{Im}(\omega(x))}{|\gamma_r-\omega(x)|^2|\gamma_k-\omega(x)|^2}\mathrm{d}x, \tag{12}$$

and $\omega(x)$ is defined as the unique solution to the following equation

$$x=\omega(x)\left(1-\frac{1}{N}\sum_{r=1}^{\bar{M}}\frac{K_r\gamma_r}{\gamma_r-\omega(x)}\right)$$

on $\{\omega\in\mathbb{C}:\mathrm{Im}(\omega)\geq 0\}$ such that $\frac{1}{N}\sum_{r=1}^{\bar{M}}\frac{K_r\gamma_r^2}{|\gamma_r-\omega(x)|^2}\leq 1$. The derivative of $\omega(x)$ with respect to x is given by

$$\omega'(x)=\frac{\partial\omega(x)}{\partial x}=\left(1-\frac{1}{N}\sum_{r=1}^{\bar{M}}\frac{K_r\gamma_r^2}{(\gamma_r-\omega(x))^2}\right)^{-1}.$$

It is assumed that $\boldsymbol{\Gamma}(\bar{\boldsymbol{\theta}})$ has bounded spectral norm and that the infimum of the smallest eigenvalue of $\boldsymbol{\Gamma}(\bar{\boldsymbol{\theta}})$ is bounded away from zero uniformly in M.

Remark: Although the expression of the asymptotic covariance in (11) is very similar to the expression of the asymptotic variance in [21, Theorem 1], it is important to stress that it is not trivial to generalize the expression of the variance to the one of the covariance. The derivation of the asymptotic covariance requires a new stochastic analysis of the G-MUSIC cost function that also considers cross terms.

The real-valued integral in (12) can numerically be computed using Riemann sum of Simpson's rule. Furthermore, in the literature $\boldsymbol{\eta}(\bar{\boldsymbol{\theta}})$ is often referred to as the asymptotic mean (first order moment) of the random cost function vector $\hat{\boldsymbol{\eta}}(\bar{\boldsymbol{\theta}})$ whereas $\boldsymbol{\Gamma}(\bar{\boldsymbol{\theta}})/N$ denotes the asymptotic covariance matrix (second order moment) of $\hat{\boldsymbol{\eta}}(\bar{\boldsymbol{\theta}})$, respectively. The diagonal entries of the asymptotic covariance matrix $[\boldsymbol{\Gamma}(\bar{\boldsymbol{\theta}})]_{p,p}/N$ in (11) describe the variance of the cost function evaluated at $\hat{\eta}(\bar{\theta}_p)$ and can be interpreted as the uncertainty of the G-MUSIC cost function in (7) around its asymptotic mean $\eta(\bar{\theta}_p)$. A sketch of the proof of Theorem 1 is provided next.

5. SKETCH OF THE PROOF

The Central Limit Theorem (CLT) in Theorem 1 can be derived by establishing pointwise convergence of the characteristic function of the statistic $\sqrt{N}(\hat{\boldsymbol{\eta}}(\bar{\boldsymbol{\theta}})-\boldsymbol{\eta}(\bar{\boldsymbol{\theta}}))$ towards the characteristic function of a Gaussian random variable. According to the Cramér-Wold device [27], it is sufficient to show that the one-dimensional projection

$$\sum_{l=1}^{L}w_l\sqrt{N}\left(\hat{\eta}(\bar{\theta}_l)-\eta(\bar{\theta}_l)\right)=\sqrt{N}\boldsymbol{w}^{\mathrm{T}}\left(\hat{\boldsymbol{\eta}}(\bar{\boldsymbol{\theta}})-\boldsymbol{\eta}(\bar{\boldsymbol{\theta}})\right) \tag{13}$$

is asymptotically Gaussian distributed for any collection of real-valued bounded quantities $\boldsymbol{w}=[w_1,...,w_L]^{\mathrm{T}}\in\mathbb{R}^L$ to proof that $\sqrt{N}(\hat{\boldsymbol{\eta}}(\bar{\boldsymbol{\theta}})-\boldsymbol{\eta}(\bar{\boldsymbol{\theta}}))$ is asymptotically jointly Gaussian distributed. Furthermore, by Lévy's continuity theorem convergence in distribution of a set of random variables can be verified by establishing pointwise convergence of the characteristic functions. Let

$$\Psi(r)=\exp\left(\mathrm{j}r\sqrt{N}\boldsymbol{w}^{\mathrm{T}}\left(\hat{\boldsymbol{\eta}}(\bar{\boldsymbol{\theta}})-\boldsymbol{\eta}(\bar{\boldsymbol{\theta}})\right)\right)$$

denote the regularization function and $\mathbb{E}[\Psi(r)]$ the corresponding characteristic function of the one-dimensional projection in (13). The objective is to analyze the asymptotic behavior of the characteristic function $\mathbb{E}[\Psi(r)]$ in the asymptotic regime where $M,N\to\infty$ at the same rate by establishing convergence towards the characteristic function of a Gaussian distributed random variable with mean $\boldsymbol{w}^{\mathrm{T}}\boldsymbol{\mu}(\bar{\boldsymbol{\theta}})$ and covariance $\boldsymbol{w}^{\mathrm{T}}\boldsymbol{\Gamma}(\bar{\boldsymbol{\theta}})\boldsymbol{w}$ such that $\mathbb{E}[\Psi(r)]-\bar{\Psi}(r)\to 0$ where

$$\bar{\Psi}(r)=\exp\left(\mathrm{j}r\boldsymbol{w}^{\mathrm{T}}\boldsymbol{\mu}(\bar{\boldsymbol{\theta}})-r^2\frac{\boldsymbol{w}^{\mathrm{T}}\boldsymbol{\Gamma}(\bar{\boldsymbol{\theta}})\boldsymbol{w}}{2}\right), \tag{14}$$

with $\boldsymbol{\mu}(\bar{\boldsymbol{\theta}})=\boldsymbol{0}$ and $\boldsymbol{\Gamma}(\bar{\boldsymbol{\theta}})$ in (11). In order to develop the characteristic function $\mathbb{E}[\Psi(r)]$ of the one-dimension projection in (13) the integration by parts formula [28, 29] as well as the Nash-Poincaré inequality [29, 30] are used. The characteristic function $\mathbb{E}[\Psi(r)]$ can be approximated with $\bar{\Psi}(r)$ in (14) up to $\mathcal{O}(N^{-1/2})$ for $M,N\to\infty$ at the same rate ($M/N\to c$, $0<c<\infty$). Further details will be provided in an accompanied journal.

6. PROBABILITY OF RESOLUTION OF G-MUSIC

To analyze the threshold effect of the G-MUSIC DoA estimator the probability of resolution is examined. The threshold effect is considered as an abrupt increase in the Mean Squared Error (MSE) of the DoA estimates below a certain SNR [5, 6] and is highly relevant to characterize the field of usage of a DoA estimator.

Consider a scenario with $K=2$ sources located at θ_1 and θ_2. As a measure to assess if the G-MUSIC estimator is able to resolve both sources we evaluate the G-MUSIC cost function in (7) at both true DoAs θ_1 and θ_2 and at the mid angle $(\theta_1+\theta_2)/2$ to detect whether the cost at the true DoAs is smaller than at the mid-angle. In case the cost at both DoAs is smaller than at the mid-angle we declare

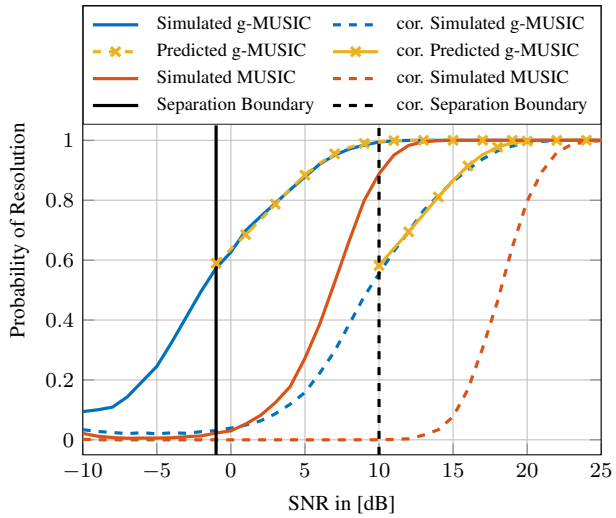

Fig. 1. Uncorrelated & Correlated Sources, Correlation coefficient ρ=0.95, Number of Sensors M=15, Number of Snapshots N=15

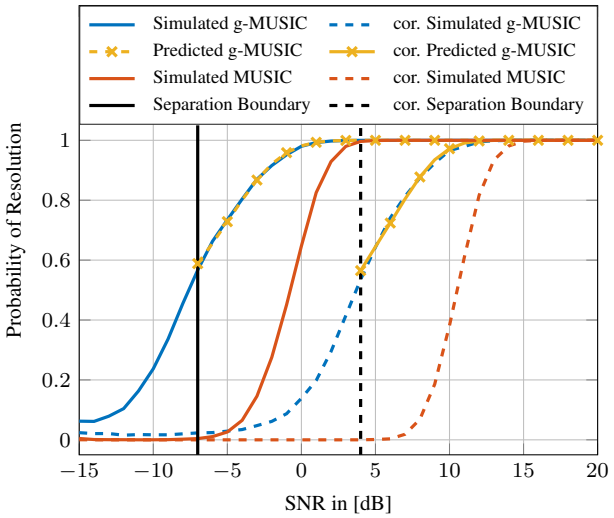

Fig. 2. Uncorrelated & Correlated Sources, Correlation coefficient ρ=0.95, Number of Sensors M=15, Number of Snapshots N=100

resolution as it is possible to distinguish between both sources [31]. In case the cost at both DoAs is larger than at the mid-angle we declare loss of resolution. Hence, the constraint to declare resolution can mathematically be expressed as $\boldsymbol{u}^{\mathrm{T}}\hat{\boldsymbol{\eta}}(\bar{\boldsymbol{\theta}})<0$ where

$$\boldsymbol{u}=\begin{bmatrix}1/2\\1/2\\-1\end{bmatrix},\quad \bar{\boldsymbol{\theta}}=\begin{bmatrix}\theta_1\\\theta_2\\\frac{\theta_1+\theta_2}{2}\end{bmatrix},\quad \hat{\boldsymbol{\eta}}(\bar{\boldsymbol{\theta}})=\begin{bmatrix}\hat{\eta}(\theta_1)\\\hat{\eta}(\theta_2)\\\hat{\eta}\left(\frac{\theta_1+\theta_2}{2}\right)\end{bmatrix}.$$

Furthermore, the asymptotic stochastic behavior of the test quantity $\boldsymbol{u}^{\mathrm{T}}\hat{\boldsymbol{\eta}}(\bar{\boldsymbol{\theta}})$ can be approximated with the previously derived asymptotic stochastic behavior of the random cost function vector $\hat{\boldsymbol{\eta}}(\bar{\boldsymbol{\theta}})$ in (10) according to

$$\sqrt{N}\boldsymbol{u}^{\mathrm{T}}\left(\hat{\boldsymbol{\eta}}(\bar{\boldsymbol{\theta}})-\boldsymbol{\eta}(\bar{\boldsymbol{\theta}})\right)\to\mathcal{N}\left(0,\boldsymbol{u}^{\mathrm{T}}\boldsymbol{\Gamma}(\bar{\boldsymbol{\theta}})\boldsymbol{u}\right),\tag{15}$$

for $M,N\to\infty$ at the same rate [32]. Consequently, the probability of resolution is computed by the cumulative distribution function

$$P_{\mathrm{res}}=\Pr\left(\boldsymbol{u}^{\mathrm{T}}\hat{\boldsymbol{\eta}}(\bar{\boldsymbol{\theta}})<0\right)=\int_{-\infty}^{0} f_{\boldsymbol{u}^{\mathrm{T}}\hat{\boldsymbol{\eta}}(\bar{\boldsymbol{\theta}})}(x)\mathrm{d}x,\tag{16}$$

where $f_{\boldsymbol{u}^{\mathrm{T}}\hat{\boldsymbol{\eta}}(\bar{\boldsymbol{\theta}})}(x)$ denotes the asymptotic probability density function (pdf) of the test quantity $\boldsymbol{u}^{\mathrm{T}}\hat{\boldsymbol{\eta}}(\bar{\boldsymbol{\theta}})$ in (15).

7. SIMULATION RESULTS

In this Section the predicted probability of resolution in (16) is compared to the simulated one. All simulations are carried out for 10000 Monte-Carlo runs. A Uniform Linear Array (ULA) that is equipped with M=15 sensors and two closely spaced sources located at $\boldsymbol{\theta}$=$[45°,50°]^{\mathrm{T}}$ are considered. The transmitted signals are zero-mean with unit power and the SNR is given by SNR=$1/\sigma^2$. The simulations are conducted for uncorrelated signals as well as correlated signal with correlation coefficient ρ=0.95. The separation boundary is defined as the smallest SNR that provides separation between the eigenvalue cluster that is associated to the noise eigenvalue γ_1 and larger adjacent eigenvalues. For SNR values smaller than the separation boundary it is not possible to distinguish between noise and signal subspace. The probability of resolution vs the SNR is depicted in Figure 1 and 2 for a scenario with N=15 and N=100 snapshots, respectively. In both scenarios the predicted probability of resolution is very close to the simulated one. Even in case of limited number of snapshots and correlated source signals the prediction of the probability of resolution is remarkably accurate.

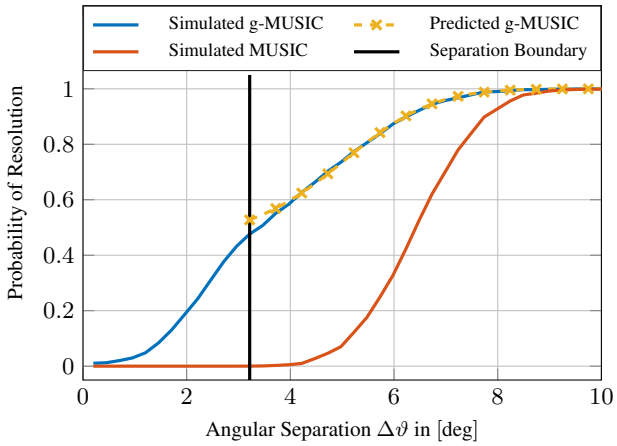

Fig. 3. Uncorrelated sources located at $\boldsymbol{\theta}$=$[45°,45°+\Delta\vartheta]^{\mathrm{T}}$, Number of Sensors M=15, Number of Snapshots N=15, SNR=2dB

Furthermore, the probability of resolution vs the angular separation $\Delta\vartheta$ between both signals for a fixed SNR of SNR=2dB and N=15 snapshots is depicted in Figure 3. The transmitted signals are uncorrelated and the two sources are located at $\boldsymbol{\theta}$=$[45°,45°+\Delta\vartheta]^{\mathrm{T}}$. The resolution capability of the G-MUSIC method for closely spaced sources is superior to the one of the conventional MUSIC method.

8. CONCLUSION

In this paper the asymptotic behavior of the G-MUSIC DoA method was investigated under the setting of RMT where both the number of snapshots and the number of sensors go to infinity at the same rate. The finite dimensional distribution of the random G-MUSIC cost function vector was derived and shown to be asymptotically jointly Gaussian distributed. The asymptotic stochastic behavior of the G-MUSIC cost function was used to predict the probability of resolution in the threshold region where the production of outliers causes a total performance breakdown.

9. REFERENCES

[1] H. Van Trees, *Optimum Array Processing: Detection, Estimation, and Modulation Theory*, Detection, Estimation, and Modulation Theory. Wiley, 2004.

[2] H. Krim and M. Viberg, "Two Decades of Array Signal Processing Research: The Parametric Approach," *IEEE Signal Processing Magazine*, vol. 13, no. 4, pp. 67–94, Jul. 1996.

[3] P.-J. Chung, M. Viberg, and J. Yu, "DOA Estimation Methods and Algorithms," vol. 3 of *Academic Press Library in Signal Processing*, pp. 599 – 650. Elsevier, 2014.

[4] R. Schmidt, "Multiple Emitter Location and Signal Parameter Estimation," *IEEE Transactions on Antennas and Propagation*, vol. 34, no. 3, pp. 276–280, Mar. 1986.

[5] D. W. Tufts, A. C. Kot, and R. J. Vaccaro, "The Threshold Analysis of SVD-based Algorithms," *IEEE International Conference on Acoustics, Speech, and Signal Processing*, vol. 4, pp. 2416–2419, 1988.

[6] D Tufts, A Kot, and R Vaccaro, "The Threshold Effect in Signal Processing Algorithms which use an Estimated Subspace," *SVD and Signal Processing II: Algorithms, Analysis and Applications*, pp. 301–320, 1991.

[7] X. Mestre and M. Á. Lagunas, "Modified Subspace Algorithms for DoA Estimation With Large Arrays," *IEEE Transactions on Signal Processing*, vol. 56, no. 2, pp. 598–614, 2008.

[8] M. Kaveh and A. Barabell, "The Statistical Performance of the MUSIC and the Minimum-Norm Algorithms in Resolving Plane Waves in Noise," *IEEE Transactions on Acoustics, Speech, and Signal Processing*, vol. 34, no. 2, pp. 331–341, 1986.

[9] B. Porat and B. Friedlander, "Analysis of the Asymptotic Relative Efficiency of the MUSIC Algorithm," *IEEE Transactions on Acoustics, Speech, and Signal Processing*, vol. 36, no. 4, pp. 532–544, 1988.

[10] P. Stoica and A. Nehorai, "MUSIC, Maximum Likelihood and Cramér-Rao Bound," *IEEE Transactions on Acoustics, Speech, and Signal Processing*, vol. 37, no. 5, pp. 720–741, May 1989.

[11] P. Stoica and A. Nehorai, "MUSIC, Maximum Likelihood and Cramér-Rao Bound: Further Results and Comparisons," *International Conference on Acoustics, Speech, and Signal Processing*, pp. 2605–2608 vol.4, May 1989.

[12] H. B. Lee and M. S. Wengrovitz, "Statistical Characterization of the MUSIC Null Spectrum," *IEEE Transactions on Signal Processing*, vol. 39, no. 6, pp. 1333–1347, Jun. 1991.

[13] Xiao-Liang Yu and K. M. Buckley, "Bias and Variance of Direction-of-Arrival Estimates from MUSIC, MIN-NORM, and FINE," *IEEE Transactions on Signal Processing*, vol. 42, no. 7, pp. 1812–1816, 1994.

[14] B. M. Radich and K. M. Buckley, "The Effect of Source Number Underestimation on MUSIC Location Estimates," *IEEE Transactions on Signal Processing*, vol. 42, no. 1, pp. 233–236, 1994.

[15] P. Vallet, X. Mestre, and P. Loubaton, "Performance Analysis of an Improved MUSIC DoA Estimator," *IEEE Transactions on Signal Processing*, vol. 63, no. 23, pp. 6407–6422, 2015.

[16] D. Schenck, X. Mestre, and M. Pesavento, "Probability of Resolution of Partially Relaxed Deterministic Maximum Likelihood: An Asymptotic Approach," *IEEE Transactions on Signal Processing*, 2020.

[17] D. Schenck, X. Mestre, and M. Pesavento, "Probability of Resolution of Partially Relaxed DML an Asymptotic Approach," *IEEE International Workshop on Computational Advances in Multi-Sensor Adaptive Processing*, pp. 410–414, 2019.

[18] D. Schenck, X. Mestre, and M. Pesavento, "Asymptotic Stochastic Analysis of Partially Relaxed DML," *IEEE International Conference on Acoustics, Speech and Signal Processing*, pp. 4920–4924, 2020.

[19] X. Mestre and P. Vallet, "On the Resolution Probability of Conditional and Unconditional Maximum Likelihood DoA Estimation," *submitted to IEEE Transactions on Signal Processing*.

[20] X. Mestre, P. Vallet, and P. Loubaton, "On the Resolution Probability of Conditional and Unconditional Maximum Likelihood DOA Estimation," *European Signal Processing Conference*, Sep. 2013.

[21] X. Mestre, P. Vallet, P. Loubaton, and W. Hachem, "Asymptotic Analysis of a Consistent Subspace Estimator for Observations of Increasing Dimension," pp. 677–680, 2011.

[22] R. Couillet and M. Debbah, *Random Matrix Methods for Wireless Communications*, Cambridge University Press, USA, 2011.

[23] X. Mestre, "Improved Estimation of Eigenvalues and Eigenvectors of Covariance Matrices Using Their Sample Estimates," *IEEE Transactions on Information Theory*, vol. 54, no. 11, pp. 5113–5129, Nov. 2008.

[24] J. W. Silverstein, "Strong Convergence of the Empirical Distribution of Eigenvalues of Large Dimensional Random Matrices," *Journal of Multivariate Analysis*, vol. 55, no. 2, pp. 331–339, Feb. 1995.

[25] V. L. Girko, "Strong Law for the Eigenvalues and Eigenvectors of Empirical Covariance Matrices," *Random Operators and Stochastic Equations*, vol. 4, no. 2, pp. 179–204, Jan. 1996.

[26] X. Mestre, "On the Asymptotic Behavior of the Sample Estimates of Eigenvalues and Eigenvectors of Covariance Matrices," *IEEE Transactions on Signal Processing*, vol. 56, no. 11, pp. 5353 – 5368, Dec. 2008.

[27] H. Wold H. Cramér, "Some Theorems on Distribution Functions," *Journal of the London Mathematical Society*, vol. 1-11, no. 4, pp. 290–294, 10 1936.

[28] W. Hachem, O. Khorunzhiy, P. Loubaton, J. Najim, and L. Pastur, "A New Approach for Mutual Information Analysis of Large Dimensional Multi-Antenna Channels," *IEEE Transactions on Information Theory*, vol. 54, no. 9, pp. 3987–4004, Sep. 2008.

[29] M. Shcherbina L. Pastur, *Eigenvalue Distribution of Large Random Matrices*, Mathematical surveys and monographs. American Mathematical Society, 2011.

[30] Louis H.Y Chen, "An Inequality for the Multivariate Normal Distribution," *Journal of Multivariate Analysis*, vol. 12, no. 2, pp. 306 – 315, 1982.

[31] Q. T. Zhang, "Probability of Resolution of the MUSIC Algorithm," *IEEE Transactions on Signal Processing*, vol. 43, no. 4, pp. 978–987, Apr. 1995.

[32] Kun Il Park, *Fundamentals of Probability and Stochastic Processes with Applications to Communications*, Springer, 2018.